ORGANIC LETTERS

2013
Vol. 15, No. 7
1548–1551

Self-Assembled Squares and Triangles by Simultaneous Hydrogen Bonding and Metal Coordination

Laura J. Marshall and Javier de Mendoza*

Institute of Chemical Research of Catalonia (ICIQ), 43007-Tarragona, Spain

jmendoza@iciq.es

Received February 4, 2013

ABSTRACT

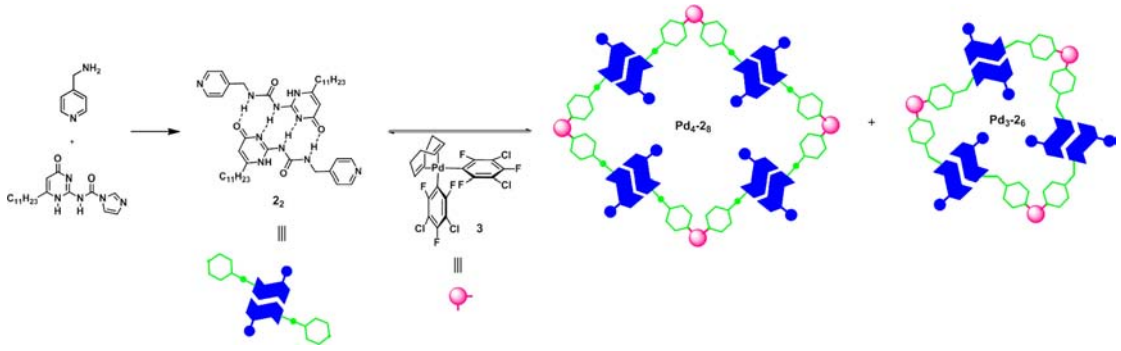

Through the combination of hydrogen bonding and metal-templated self-assembly, molecular squares and molecular triangles are observed in chloroform solution upon the complexation of hydrogen-bonded dimers of *para*-pyridyl-substituted 2-ureido-4-[1*H*]-pyrimidinone (UPy) and an appropriate *cis*-substituted palladium complex. Molecular modeling studies and NMR analysis confirmed the presence of two distinct structures in solution: the tubular structure of the molecular square and propeller-bowl structure of the molecular triangle.

Hydrogen bonding has been widely employed to build up rosette-like supramolecular structures.[1,2] Use of cyanuric acid−melamine combinations,[3] hydrogen bond scaffolds inspired by G−C pairs,[4] or G-quartet mimics,[5] among others,[6] have been reported. Also, 2-ureido-4-[1*H*]-pyrimidinone (UPy) has been efficiently employed to build up self-assembled architectures,[7] due to the remarkable strength of the dimers arising from its DDAA hydrogen bonding array [K_a(chloroform) > 10^7 M^{-1}].[8] We recently reported a 16 hydrogen bonded self-assembly of tubular

(1) (a) Lindoy, L. F.; Atkinson, I. M. *Self-assembly in Supramolecular Systems*; Royal Society of Chemistry: Cambridge, 2000. (b) Lehn, J.-M. *Science* **2002**, *295*, 2400. (c) Whitesides, G. M.; Grzybowski, B. *Science* **2002**, *295*, 2418. (d) Philp, D.; Stoddart, J. F. *Angew. Chem., Int. Ed. Engl.* **1996**, *35*, 1154.

(2) For a discussion on the factors that favor rosettes over open-chain oligomers, see: Ballester,P. and de Mendoza, J. In *Modern Supramolecular Chemistry: Strategies for Macrocycle Synthesis*; Diederich, F., Stang, P. J., Tykwinski, R. R., Wiley−VCH: Weinheim, 2008; pp 69.

(3) For reviews on cyanuric acid−melamine rosettes, see: (a) Whitesides, G. M.; Simanek, E. E.; Mathias, J. P.; Seto, C. T.; Chin, D. N.; Mammen, M.; Gordon, D. M. *Acc. Chem. Res.* **1995**, *28*, 37. (b) Prins, L. J.; Reinhoudt, D. N.; Timmerman, P. *Angew. Chem., Int. Ed.* **2001**, *40*, 2382. (c) Mateos-Timoneda, M. A.; Crego-Calama, M.; Reinhoudt, D. N. *Chem. Soc. Rev.* **2004**, *33*, 363.

(4) (a) Marsh, A.; Silvestri, M.; Lehn, J.-M. *Chem. Commun.* **1996**, 1527. (b) Mascal, M.; Hext, N. M.; Warmuth, R.; Moore, M. H.; Turkenburg, J. P. *Angew. Chem., Int. Ed. Engl.* **1996**, *35*, 2204. (c) Kolotuchin, S. V.; Zimmerman, S. C. *J. Am. Chem. Soc.* **1998**, *120*, 9092. (d) Ma, Y.; Kolotuchin, S. V.; Zimmerman, S. C. *J. Am. Chem. Soc.* **2002**, *124*, 13757. (e) Fenniri, H.; Deng, B. L.; Ribbe, A. E. *J. Am. Chem. Soc.* **2002**, *124*, 11064. (f) Johnson, R. S.; Yamazaki, T.; Kovalenko, A.; Fenniri, H. *J. Am. Chem. Soc.* **2007**, *129*, 5735.

(5) For reviews on G-quartets, see: (a) Davis, J. T. *Angew. Chem., Int. Ed.* **2004**, *43*, 668. (b) Davis, J. T.; Spada, G. P. *Chem. Soc. Rev.* **2007**, *36*, 296.

(6) (a) Corbin, P. S.; LawlessQQ, L. J.; Li, Z.; Ma, Y.; Witmer, M. J.; Zimmerman, S. C. *Proc. Natl. Acad. Sci. U.S.A.* **2002**, *99*, 5099. (b) Todd, E. M.; Zimmerman, S. C. *Tetrahedron* **2008**, *64*, 8558.

(7) (a) González, J. J.; Prados, P.; de Mendoza, J. *Angew. Chem., Int. Ed.* **1999**, *38*, 525. (b) Keizer, H. M.; González, J. J.; Segura, M.; Prados, P.; Sijbesma, R. P.; Meijer, E. W.; de Mendoza, J. *Chem.—Eur. J.* **2005**, *11*, 4602. (c) Hahn, U.; González, J. J.; Huerta, E.; Segura, M.; Eckert, J.-F.; Cardinali, F.; de Mendoza, J.; Nierengarten, J.-F. *Chem.—Eur. J.* **2005**, *11*, 6666. (d) Huerta, E.; Metselaar, G. A.; Fragoso, A.; Santos, E.; Bo, C.; de Mendoza, J. *Angew. Chem., Int. Engl.* **2007**, *46*, 202. (e) Huerta, E.; Cequier, E.; de Mendoza, J. *Chem. Commun.* **2007**, 5016.

(8) (a) Sijbesma, R. P.; Beijer, F. H.; Brunsveld, L.; Folmer, B. J. B.; Hirschberg, J. H. K. K.; Lange, R. F. M.; Lowe, J. K. L; Meijer, E. W. *Science* **1997**, *278*, 1601. (b) Söntjens, S. H. M.; Sijbesma, R. P.; van Genderen, M. H. P.; Meijer, E. W. *J. Am. Chem. Soc.* **2000**, *122*, 7487.

10.1021/ol400326r
Published on Web 03/18/2013

cyclic tetramers based on UPy subunits attached to a 3,6-carbazolyl core, in which substituents are oriented to both edges of the ring to improve the solubility of the aggregate.[9]

Alternatively, self-assembly into helices, macrocycles, and cages can be achieved through metal coordination. Independent work pioneered by Fujita and Stang, utilizing square planar Pd(II) or Pt(II) metal centers coordinated to 4,4′-bypyridine ligands, generates charged, cyclic frameworks.[10−12] The combination of the 90° angle of the *cis*-coordinated metal centers with the 180° angle of the linear ligand provides the basis for the square framework. Fujita also reported molecular triangles in solution, depending on the length and flexibility of the ligands, with short inflexible ligands more likely to form squares than longer, flexible ones, which often result in a square-triangle equilibrium.

We reasoned that the substitution of our carbazolyl moiety[9] for a square planar *cis*-coordinated Pd(II) species would favor the formation of neutral tetrameric cyclic arrangements, each UPy dimer constituting an edge and each metal center a corner (Figure 1). To the best of our knowledge, the combination of both hydrogen bonding and metal-templated self-assembly, without interference, for the formation of discrete cyclic molecular squares and triangles has never been reported.[13,14] As we previously observed,[9] the presence of a methylene spacer between the carbazole and the UPy moieties was essential for the formation of cyclic aggregates.

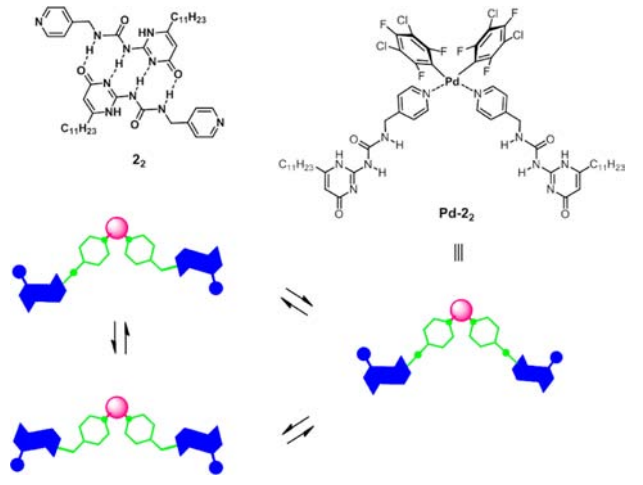

Figure 1. *Para*-substituted UPy dimer $\mathbf{2_2}$ (edge), two monomers of **2** coordinated to the Pd(II) species **Pd-2$_2$**, and schematic representation of conformations around the UPy subunits.

Initially, we prepared compound **1** with no methylene spacer between the UPy and pyridyl moieties (see Supporting Information (SI)). However, this compound was not soluble in $CDCl_3$, except in the presence of a trace of trifluoroacetic acid (TFA), and no dimers were observed by ^{1}H NMR spectroscopy under these conditions. The formation of dimers was also unsuccessful in tetrahydrofuran (THF). In contrast, dimer $\mathbf{2_2}$ bearing the methylene spacer for increased flexibility showed the well-defined, typical signature for a UPy dimer in ^{1}H NMR ($CDCl_3$, sharp peaks at 12.97, 12.17, and 11.04 ppm).[7,9,15] The addition of traces of TFA allowed characterization of the monomeric species **2**.

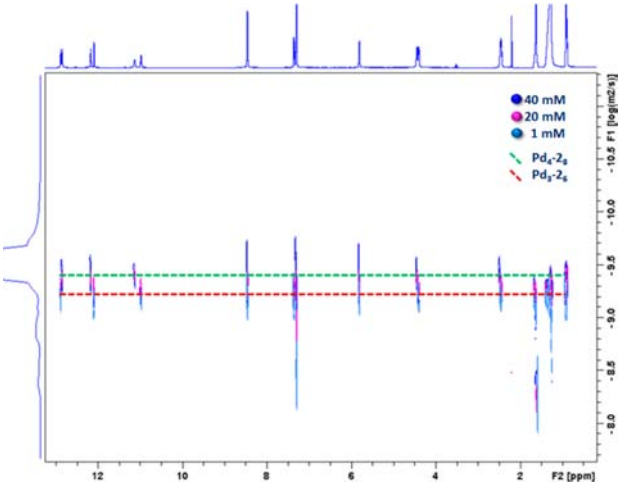

Figure 2. DOSY spectra of aggregates **Pd$_3$-2$_6$** and **Pd$_4$-2$_8$** ($CDCl_3$) at 1 mM (light blue), 20 mM (pink), and 40 mM (dark blue).

From the variety of *cis*-protected square planar palladium(II) complexes tested for complexation to the dimer (solubility, ^{1}H and ^{19}F NMR analysis), only (1,5-cyclooctadiene)bis-(3,5-dichloro-2,4,6-trifluorobenzene) palladium(II) **3** was found to be successful. Upon mixing equimolecular amounts of $\mathbf{2_2}$ and **3**, shifts were observed in the hydrogen-bonding and pyridyl regions of the ^{1}H NMR spectra,

(9) Yang, Y.; Xue, M.; Marshall, L. J.; de Mendoza, J. *Org. Lett.* **2011**, *13*, 3186.

(10) (a) Fujita, M.; Sasaki, P. O.; Mitsuhashi, T.; Fujita, J.; Yazaki, K.; Yamaguchi, K.; Ogura, K. *Chem. Commun.* **1996**, 1535. (b) Fujita, M.; Yazaki, J.; Ogura, K. *J. Am. Chem. Soc.* **1990**, *112*, 5645. (c) Stang, P. J.; Cao, D. H. *J. Am. Chem. Soc.* **1994**, *116*, 4981.

(11) Recent reviews: (a) Yoshizawa, M.; Klosterman, J. K.; Fujita, M. *Angew. Chem., Int. Ed.* **2009**, *48*, 3418. (b) Cook, T. R.; Zheng, Y.-R.; Stang, P. J. *Chem. Rev.* **2013**, *113*, 734.

(12) For other recent examples, see: (a) Hess, J. L.; Hseih, C.-H.; Brothers, S. M.; Hall, M. B.; Darensbourg, M. Y. *J. Am. Chem. Soc.* **2011**, *133*, 20426. (b) Karthikeyan, S.; Velavan, K.; Sathishkumar, R.; Varghese, B.; Manimaran, B. *Organometallics* **2012**, *31*, 1952.

(13) For further examples of orthogonality in supramolecular chemistry, see: (a) Huck, W. T. S.; Hulst, R.; Timmerman, P.; van Veggel, F. C. J. M.; Reinhoudt, D. N. *Angew. Chem., Int. Ed. Engl.* **1997**, *36*, 1006. (b) Wong, C.-H.; Zimmerman, S. C. *Chem. Commun.* **2013**, *49*, 1679.

(14) For a combination of metals and hydrogen bonds in dimeric capsules, see: (a) Yamanaka, M.; Toyoda, N.; Kobayashi, K. *J. Am. Chem. Soc.* **2009**, *131*, 9880–9881. (b) Yamanaka, M.; Kawaharada, M.; Nito, Y.; Takaya, H.; Kobayashi, K. *J. Am. Chem. Soc.* **2011**, *133*, 16650.

(15) (a) Sijbesma, R. P.; Beijer, F. H.; Brunsveld, L.; Folmer, B. J. B.; Hirschberg, J. H. K. K.; Lange, R. F. M.; Lowe, J. K. L; Meijer, E. W. *Science* **1997**, *278*, 1601. (b) Beijer, F. H.; Kooijman, H.; Spek, A. L.; Sijbesma, R. P.; Meijer, E. W. *Angew. Chem., Int. Ed.* **1998**, *110*, 79. (c) Söntjens, S. H. M.; Sijbesma, R. P.; van Genderen, M. H. P.; Meijer, E. W. *J. Am. Chem. Soc.* **2000**, *122*, 7487.

as well in the ^{19}F NMR spectra, corresponding to the fluorine atoms on the Pd ligands.

Two species displaying a high level of symmetry at room temperature were observed. Variable concentration ^{1}H DOSY diffusion experiments in $CDCl_3$ (Figure 2) confirmed the presence of two discrete species of different sizes (observation of two well-defined signals on the *D* axis). The spectra show the slight change of *D* with the concentration increase, which favors cyclic oligomers.[2] Using the Stokes–Einstein equation, the experimentally found diffusion coefficients of the two species were converted to approximate hydrodynamic radii.[16] Thus, values of 8.9 and 6.4 Å at 20 mM for the large and small species respectively were calculated, translating into "spherical" volumes of 3070 and 1148 Å^3. The average theoretically estimated radii/volumes for a square (9.9 Å/4064 Å^3) and triangle (6.7 Å/1260 Å^3) strongly point toward these two species being present in solution (pentamer > 5000 Å^3).[17–19]

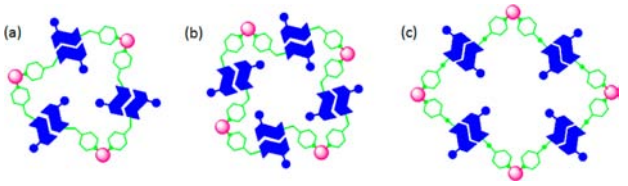

Figure 3. Schematic representation of cyclic aggregates from $\mathbf{2_2}$ and **3**. (a) Propeller-shaped triangle. (b) Propeller-shaped square. (c) Tubular-shaped tetramer.

The assembly of flat, rosette-like structures (schematically shown in Figure 3) is unlikely, as it would result in significant torsional strain, and subsequent unfavorable hydrogen-bonding angles, due to the presence of the undecyl chains at the inner region of the rosette, as clearly revealed by model inspection. In contrast, folded structures can easily be arranged. Indeed, model optimizations[18] for the triangle are fully compatible with a propeller-like shape (at 25 °C) or a bowl-shaped aggregate (at low temperature) where both UPy subunits in each monomer are pointing to opposite sides (Figures 3a and 4). In the case of the square, although a propeller-like structure is also possible (Figure 3b), model optimizations suggest that a very favorable, sterically unhindered tubular (belt-like) shape can be generated (Figures 3c and 5), as with our carbazole tetramer.[9] In this case both UPy subunits are mirror images pointing to the same side of the spacer and all alkyl chains orient away from the assembly, and into the bulk solvent.

(16) $r_h = k_bT/(6\pi\eta D)$, in which the solute is a spherical species.

(17) Theoretical values can be approximately calculated by taking the average of the length, width, and height of the dissolved species, as measured on the optimized models for the different cyclic oligomers.

(18) Structures were minimized in vacuo by molecular mechanics using Augmented MM3 parameters (OG_MM-MM3 protocol) within the SCIGRESS 7.7.0.47 software (Fujitsu Ltd.).

(19) Timmerman, P.; Weidmann, J.-L.; Jollife, J. A.; Prins, L. J.; Reindhoudt, D. N.; Shinkai, S.; Frish, L.; Cohen, Y. *J. Chem. Soc., Perkin Trans. 2* **2000**, 2077.

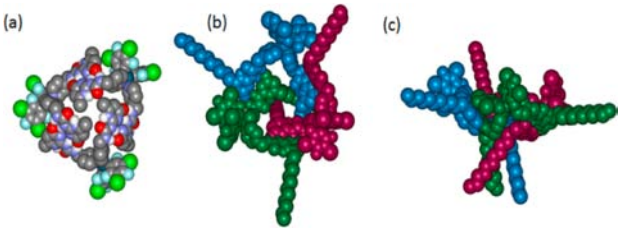

Figure 4. Optimized CPK models of molecular triangle $\mathbf{Pd_3\text{-}2_6}$ showing the bowl-shaped aggregate. (a) Bottom view omitting undecyl chains (colored by atom type). (b) Top view showing undecyl chains (colored by unit $\mathbf{Pd\text{-}2_2}$). (c) Side view showing orientation of undecyl chains.

Further spectroscopic studies were in full agreement with our predictions of the presence of a molecular square and a molecular triangle (see SI for spectra). For instance, at lower concentrations (~1 mM) the triangle was present in greater abundance, with the amount of the square increasing linearly as concentration was increased, as expected (DOSY).

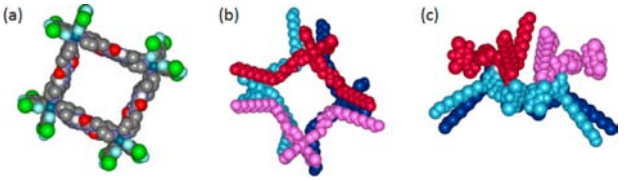

Figure 5. Optimized CPK models of molecular square $\mathbf{Pd_4\text{-}2_8}$ showing the tubular-shaped aggregate. (a) Top view omitting undecyl chains (colored by atom type). (b) Top view showing undecyl chains (colored by unit $\mathbf{Pd\text{-}2_2}$). (c) Side view.

Variable temperature ^{1}H and ^{19}F NMR studies confirmed that the aggregates were destroyed at high temperatures (> 378 K). Upon increasing the temperature, formation of the entropically more stable, but enthalpically less stable, triangle was favored. Upon lowering the temperature the enthalpically more stable square was observed. It is also likely that, at low temperatures, where both species are less flexible, the bowl shaped triangle is more sterically hindered than the tubular square species and is, therefore, less favorable.[10,11]

NOESY spectra at 298 K ($CDCl_3$) give little information regarding the conformation of the two species, as all aggregates are dynamic at room temperature. However, one NH proton of each species (10.96 and 11.12 ppm for the triangle and square respectively) does not show contacts with the first CH_2 of the undecyl chain. However at 213 K, where the structures are "frozen", the NH proton at 10.96 ppm shows contacts with both the first methylene group of the undecyl chain and the UPy CH proton (5.80 ppm) of its dimeric partner. Generally the NH protons of

the triangular species show greater interactions with the protons of the undecyl chain than the square due to their closer proximity at lower temperatures. These interactions are not observed in the square, thus confirming that at lower temperatures the triangular species is likely to adopt the bowl conformation, whereas in the square the tubular arrangement (Figure 5) prevails, as in our carbazole tetramer,[9] with both hydrogen bonded edges oriented in a similar way as the 4,4′-bypyridine ligands of Fujita's squares.[10,11] As our "edges" are longer and more flexible than 4,4′-bipyridine, this also accounts for the observation of both squares and triangles in solution.

In order to examine the effect of the angle between the two pyridyl-UPy substituents on the metal center, dimer $\mathbf{4_2}$ was prepared, where a *meta*-substituted pyridine center is utilized. This is likely to increase the angle between the UPy substituents (Figure 6a), as the other conformations (Figures 6b–c) are not likely to be observed due to steric reasons.

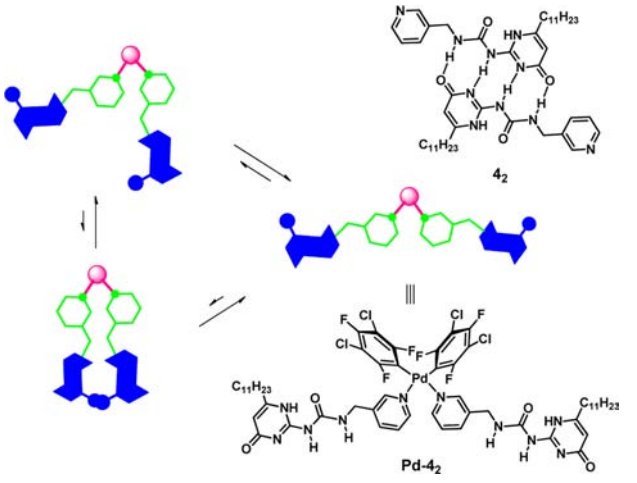

Figure 6. *Meta*-substituted UPy dimer $\mathbf{4_2}$, two monomers of **4** coordinated to the Pd(II) species (**Pd-4$_2$**), and schematic representation of conformations around the UPy subunits.

Since the angle is closer to 180° than in the *para*-substituted compounds (~90°), it is possible that oligomeric or polymeric species may form. Indeed dimers were observed in solution ($CDCl_3$) for $\mathbf{4_2}$, and a discrete species formed upon addition of the palladium species **3**, as sharp signals were observed in the ^{1}H NMR spectrum. At lower concentrations (1 mM) two species were present in equal amounts, but at a higher concentration (< 40 mM) the intensity of the signals of only one species increased. As expected, variable temperature ^{1}H and ^{19}F NMR studies showed that increasing the temperature above 378 K resulted in the destruction of the aggregates. In the ^{1}H NMR spectrum at low temperatures a small splitting was observed in the NH signal at 11.11 ppm and the CH_2 signal at 4.38 ppm (corresponding to the methylene spacer). This suggests not only that these two protons are coupling to one another but also that the environments of the two protons on the methylene spacer are nonequivalent at low temperatures.

DOSY diffusion experiments (1–40 mM, $CDCl_3$) and use of the Stokes–Einstein equation yielded an approximate hydrodynamic radius of only 5.3 Å, giving a "spherical" volume of 670 Å^3. This value is too small to represent any discrete cyclic aggregate. For the monomeric species (after addition of TFA) an approximate hydrodynamic radius of 3.7 Å (212 Å^3) was calculated. This suggests a dynamic mixture of small hydrogen-bonded and metal-coordinated species in solution, which are equivalent on the NMR time scale at room temperature. The ^{19}F NMR spectrum shows the presence of more than one signal for both the *ortho*- and *para*-fluorine atoms, further suggesting that more than one species is present. Also, low temperature NMR studies confirm the lower symmetry of these species compared to the discrete cyclic aggregates.

An attempt to reduce the length of the chains (butyl instead of undecyl) of the *meta*-substituted species to favor cyclic aggregates (see SI for compounds **5**, **Pd$_4$-5$_8$**, and **Pd$_3$-5$_6$**) resulted in poor solubility. Finally, complexation of dimeric species $\mathbf{2_2}$ with a platinum complex instead of a palladium one was attempted but this was unsuccessful.

In summary, we have demonstrated that through hydrogen bonding (UPy dimers) and metal coordination (Pd-pyridine), self-assembly occurs in chloroform solution to form neutral molecular squares and triangles, without interference of both supramolecular interactions. As expected, the process is sensitive to slight structural changes relating to internal angles, steric factors, and solubility issues, highlighting the need for careful design in these types of systems.[9] These results pave the way for the design of more complex molecular architectures by the combination of hydrogen bonding and metal complexation.

Acknowledgment. The Ministry of Economy and Competitivity (MINECO, Spain) (Projects CTQ2008-00183 and CTQ2011-28677), the ICIQ Foundation, and Consolider Ingenio (Grant 2010 CSD 2006-0003) are kindly acknowledged.

Supporting Information Available. Experimental details, characterization, and spectral data. This material is available free of charge via the Internet at http://pubs.acs.org.

The authors declare no competing financial interest.